Molecular Vision 2017; 23:228-241 <http://www.molvis.org/molvis/v23/228>
Received 30 November 2016 | Accepted 12 April 2017 | Published 14 April 2017

Early AMD-like defects in the RPE and retinal degeneration in aged mice with RPE-specific deletion of *Atg5* or *Atg7*

Youwen Zhang,[1] Samuel D. Cross,[1] James B. Stanton,[2] Alan D. Marmorstein,[1] Yun Zheng Le,[3] Lihua Y. Marmorstein[1]

[1]Department of Ophthalmology, Mayo Clinic, Rochester, MN; [2]Department of Ophthalmology & Vision Science, University of Arizona, Tucson, AZ; [3]Department of Medicine and Harold Hamm Diabetes Center, University of Oklahoma Health Sciences Center, Oklahoma City, OK

Purpose: To examine the effects of autophagy deficiency induced by RPE-specific deletion of *Atg5* or *Atg7* in mice as a function of age.

Methods: Conditional knockout mice with a floxed allele of *Atg5* or *Atg7* were crossed with inducible *VMD2-rtTA/Cre* transgenic mice. *VMD2*-directed RPE-specific Cre recombinase expression was induced with doxycycline feeding in the resulting mice. Cre-mediated deletion of floxed *Atg5* or *Atg7* resulted in RPE-specific inactivation of the *Atg5* or *Atg7* gene. Plastic and thin retinal sections were analyzed with light and electron microscopy for histological changes. Photoreceptor outer segment (POS) thickness in plastic sections was measured using the Adobe Photoshop CS4 extended ruler tool. Autophagic adaptor p62/SQSTM1 and markers for oxidatively damaged lipids, proteins, and DNA were examined with immunofluorescence staining of cryosections. Fluorescence signals were quantified using Image J software.

Results: Accumulation of p62/SQSTM1 reflecting autophagy deficiency was observed in the RPE of the $Atg5^{\Delta RPE}$ and $Atg7^{\Delta RPE}$ mice. 3-nitrotyrosine, advanced glycation end products (AGEs), and 8-hydroxy-2'-deoxyguanosine (8-OHdG), markers for oxidatively damaged proteins and DNA, were also found to accumulate in the RPE of these mice. We observed retinal degeneration in 35% of the $Atg5^{\Delta RPE}$ mice and 45% of the $Atg7^{\Delta RPE}$ mice at 8 to 24 months old. Degeneration severity and the number of mice with degeneration increased with age. The mean POS thickness of these mice was 25 µm at 8–12 months, 15 µm at 13–18 months, and 3 µm at 19–24 months, compared to 35 µm, 30 µm, and 24 µm in the wild-type mice, respectively. Early age-related macular degeneration (AMD)-like RPE defects were found in all the $Atg5^{\Delta RPE}$ and $Atg7^{\Delta RPE}$ mice 13 months old or older, including vacuoles, uneven RPE thickness, diminished basal infoldings, RPE hypertrophy/hypotrophy, pigmentary irregularities, and necrosis. The severity of the RPE defects increased with age and in the mice with retinal degeneration. RPE atrophy and choroidal neovascularization (CNV) were occasionally observed in the $Atg5^{\Delta RPE}$ and $Atg7^{\Delta RPE}$ mice with advanced age.

Conclusions: Autophagy deficiency induced by RPE-specific deletion of *Atg5* or *Atg7* predisposes but does not necessarily drive the development of AMD-like phenotypes or retinal degeneration.

The RPE plays an essential role in supporting photoreceptor function. One critical role of the RPE is to dispose of waste products from photoreceptors [1,2]. RPE cells are postmitotic and are subjected to lifelong exposure to high levels of oxidative stress. The lack of RPE cell turnover requires that RPE cells adapt efficient systems to limit environmental damage. This includes the ubiquitin-proteasome system and autophagy as a means of eliminating damaged cellular components. While the proteasome system predominantly degrades misfolded proteins and requires substrates to be unfolded to pass through the narrow pore of the proteasomal barrel, autophagy is a potent lysosomal degradation pathway capable of the disposal of bulk damaged macromolecular complexes and organelles [3,4].

Correspondence to: Lihua Y. Marmorstein, Department of Ophthalmology, Mayo Clinic, 200 1st St. SW, Rochester, MN; Phone: (507) 284 2248; FAX: (507) 284 8566; email: Marmorstein.Lihua@mayo.edu

Three forms of autophagy have been identified: macroautophagy, chaperone-mediated autophagy, and microautophagy [5]. Autophagy typically refers to macroautophagy, the major catabolic mechanism used by eukaryotic cells to degrade long-lived proteins, lipids, and organelles [5]. More than 30 *ATG* (AuTophaGy) genes that execute or regulate autophagy have been identified from yeast to mammals [5]. Autophagy occurs at low basal levels in virtually all cells to perform essential homeostatic functions but is rapidly upregulated when cells need to eliminate damaging cytoplasmic components or intracellular pathogens [6]. In general, it is accepted that autophagy function declines with age since a common characteristic of all aging cells is the accumulation of macromolecules and organelles [6]. This occurs even in the absence of any mutations that predispose the cells to a pathogenic phenotype, such as aggregation-prone mutant proteins [4,6,7]. The accumulation of altered components is particularly detrimental in non-dividing cells, such as

neurons. Overwhelming evidence indicates that autophagy is protective against neurodegeneration in a wide range of neuronal degenerative diseases [3,6,8-10].

The high oxygen environment of the outer retina results in an enormous amount of oxidized waste that needs to be removed to preserve vision. As an example, the RPE phagocytoses 10% of the volume of the photoreceptor outer segment (POS) every day [1]. Even under normal circumstances, the autophagic capacity of RPE cells is burdened by this immense amount of metabolic waste [11]. Lipofuscin (highly cross-linked aggregates of oxidized proteins and lipids) and other waste products generated through phagocytosis and other physiologic processes accumulate in the RPE early in life and increase with age [11,12]. This accumulation is thought to play a role in age-related macular degeneration (AMD) by imposing an increasing burden on RPE cells. For this reason, it can be hypothesized that any impairment of autophagy could be detrimental to the cellular functions of the RPE. In support of this hypothesis, it has been reported that autophagy dysfunction in the RPE is associated with the pathogenesis of AMD and other forms of retinal degeneration [13-19]. Importantly, markers of autophagy have been found in drusen, a form of sub-RPE deposits associated with AMD, as well as in aged human and mouse RPE, Bruch's membrane, and the choroid [15,18,20]. RPE cells in AMD are often engorged with lipofuscin and damaged organelles [6,12,21,22]. A common early feature of AMD is the presence of sub-RPE deposits accompanied by RPE hypertrophy [21,23,24]. RPE geographic atrophy and choroidal neovascularization (CNV) define the late stages of AMD [21,24]. Although it is not understood how sub-RPE deposits are formed, all of the deposits contain common components, including oxidized proteins, lipids, DNA, ubiquitin, advanced glycation end products (AGEs), membrane and cellular debris, vacuoles, and inflammation-related proteins [7,25,26]. Proteins modified by products of lipid peroxidation or glucoxidation, such as 4-hydroxynonenal (HNE), carboxyethyl pyrrole (CEP), or AGEs, are found in lipofuscin granules or sub-RPE deposits associated with AMD [8,12,27]. It has been postulated that faulty degradative processes in the RPE may account for their accumulation and the deposits instigate chronic local inflammation [8,21,28,29].

ATG5 and ATG7 are two core components of the autophagy machinery and are so essential for autophagy function that *Atg5*$^{-/-}$ and *Atg7*$^{-/-}$ mice die shortly after birth [5,30-32]. Conditional knockout of *Atg5* in mouse RPE has shown that the interplay of phagocytosis and autophagy in an Atg5-dependent manner is required for POS degradation and the maintenance of retinoid levels to support vision [33]. RPE-specific deletion of *Atg7* in mice indicates that autophagy is important in maintaining RPE homeostasis [34,35]. As dysfunction of the RPE becomes progressively worse with age, and retinal degenerative changes progress with age, the goal of this study was to investigate the impact of RPE-specific deletion of *Atg5* or *Atg7* in the retina as a function of age.

METHODS

Mice: Conditional knockout mice with floxed alleles of *Atg5* (*Atg5*$^{flox/flox}$) *or Atg7* (*Atg7*$^{flox/flox}$) were obtained from the RIKEN BioResource Center (Koyadai, Ibaraki, Japan). The *Atg5*$^{flox/flox}$ mice were generated by Dr. Noboru Mizushima [36]. The *Atg7*$^{flox/flox}$ mice were generated by Dr. Masaaki Komatsu [32]. These mice were crossed with *VMD2-rtTA/cre* transgenic mice [37] to generate mice with inducible RPE-specific deletion of *Atg5* or *Atg7.* The transgenic mice carry the human *vitelliform macular dystrophy 2* (*VMD2*) promoter-directed *reverse tetracycline-dependent transactivator* (*rtTA*), and the tetracycline-responsive element-directed *cre* gene [37]. *VMD2* is an older name for the *BEST1* (Gene ID: 7439; OMIM 607854) gene that has been replaced by the Human Genome Organization (HUGO) nomenclature committee. Bestrophin 1, the protein encoded by *VMD2/BEST1*, has been shown by us to localize specifically to RPE cells [38], and the *VMD2* promoter directs RPE-specific gene expression [39]. Strain background can affect the phenotype of genetically modified mice [40], so we crossed these mice with a pigmented (C57BL/6J) or albino (Balb/c) background. The mice were backcrossed eight times to each background. *VMD2*-directed RPE-specific Cre recombinase expression was induced with doxycycline (Sigma Aldrich, St. Louis, MO) feeding for 1 week after the mice were born. Doxycycline is light sensitive and was administered in the drinking water at a dose of 0.2 mg/ml in amber water battles. Cre-mediated deletion of floxed *Atg5* or *Atg7* fragments results in RPE-specific inactivation of the *Atg5* (*Atg5*$^{\Delta RPE}$) or *Atg7* (*Atg7*$^{\Delta RPE}$) gene. Neither the transgenes nor the inducing drugs have an adverse effect on the health of the retina [37]. All mice were handled in accordance with the ARVO Statement for the Use of Animals in Ophthalmic and Vision Research, using protocols approved by the Institutional Animal Care and Use Committee of the University of Arizona or Mayo Clinic. Other than doxycycline induction, the mice were housed in standard conditions and maintained on a 12 h:12 h light-dark cycle with free access to water and food.

PCR analysis of isolated RPE cells: PCR was performed with DNA extracted from isolated RPE cells to confirm the floxed *Atg5* or *Atg7* fragment is deleted in the RPE of *Atg5*$^{\Delta RPE}$ or

Atg7$^{\Delta RPE}$ mice. The neuroretina was used as a positive control. To isolate the RPE cells, the mice were euthanized with CO_2 asphyxiation, and the eyes were enucleated. A circumferential incision was made posterior to the limbus and the anterior segments removed. The neurosensory retina was carefully peeled from the eyecup. The RPE was exposed after the neurosensory retina was removed. With the optic nerve head at the center of the eyecup, four radial cuts were made in the eyecup to flatten it. RPE sheets were gently scraped from Bruch's membrane with a #15 scalpel blade. For the *Atg5*$^{\Delta RPE}$ mice, PCR primers (A, 5′-GAA TAT GAA GGC ACA CCC CTG AAA TG-3′; B, 5′-GTA CTG CAT AAT GGT TTA ACT CTT GC-3′; C, 5′-ACA ACG TCG AGC ACA GCT GCG CAA GG-3′; D, 5′-CAG GGA ATG GTG TCT CCC AC-3′; E, 5′-AGG TTC GT TCA CTC ATG GA-3′; F, 5′-TCG ACC AGT TTA GTT ACC C-3′) described by Hara et al. were used [36]. For the *Atg7*$^{\Delta RPE}$ mice, PCR was performed using the primers (1, 5′-TGG CTG CTA CTT CTG CAA TGA TGT-3′; 2, 5′-GAA GGG ACT GGC TGC TAT TGG GCG AAG TGC-3′; and 3, 5′-TTA GCA CAG GGA ACA GCG CTC ATG G-3′) described by Komatsu et al. [32].

Reverse transcription polymerase chain reaction (RT-PCR) was performed (1 µl of RT samples was used for a 25-µl PCR reaction) as previously described [41] to confirm the absence of *Atg5* or *Atg7* mRNA expression in the RPE of the *Atg5*$^{\Delta RPE}$ or *Atg7*$^{\Delta RPE}$ mice. The neuroretina was used as a positive control. For the *Atg5*$^{\Delta RPE}$ mice, the primers for RT–PCR were 5′-GAT GTG CTT CGA GAT GTG TG-3′ and 5′-CTG GGT AGC TCA GAT GCT CG-3′. For the *Atg7*$^{\Delta RPE}$ mice, the primers for RT–PCR were 5′-CAA CAT GAG CAT CCC CAT GC-3′ and 5′-AGG TGA ATC CTT CTC GCT CG-3′. *Efemp1* primers [40] were used in the control.

Immunofluorescence: The mice were euthanized, and the eyes were dissected and fixed in 4% paraformaldehyde (pH 7.4) in 0.1 M phosphate buffer at 4 °C for 4 h. The fixed eyes were cryoprotected in 20% sucrose and embedded in optimum cutting temperature (OCT; Thermo Fisher Scientific, Waltham, MA) at −20 °C. Immunofluorescence staining of the 10 µm frozen sections was performed as previously described [42] using a rabbit polyclonal antibody against HNE (Abcam, Cambridge, MA), malondialdehyde (MDA; Abcam), AGEs (Abcam), or p62/SQSTM1 (MBL International, Woburn, MA), or a mouse monoclonal antibody against 3-nitrotyrosine (39B6, Abcam), or 8-OHdG (15A3, Santa Cruz, Dallas, TX). A goat anti-rabbit immunoglobulin G (IgG) or anti-mouse IgG Alexa Fluor 488 conjugate was used as a secondary antibody (Invitrogen, Carlsbad, CA). Cell nuclei were stained with 4',6-diamidino-2-phenylindole (DAPI). The sections were examined and photographed using a Nikon E600 (Melville, NY) microscope equipped with a charge coupled device (CCD) camera.

Quantification of fluorescence intensities was performed using ImageJ software (National Institutes of Health, Bethesda, MD). Sections from three mice (n = 3) per genotype were used. Three images taken from the three randomly selected areas in each stained section were measured. In each image, the outline of the RPE layer was drawn, and the area, mean fluorescence, and background readings were measured. The total RPE fluorescence was calculated as integrated density − (area of selected sections × mean fluorescence of background readings). Data are reported as mean ± standard deviation (SD; $p < 0.05$).

Histological analysis: Mouse eyes were fixed in 4% paraformaldehyde/2% glutaraldehyde in 0.1 M phosphate buffer (pH 7.2) overnight. The tissues were processed as previously described [42]. One micron plastic sections were stained with toluidine blue. Sixty nanometer thin sections were examined and photographed using a JEM1400 electron microscope (JEOL USA, Peabody, MA) equipped with a Gatan Ultrascan 1000XP CCD camera (Gatan, Pleasanton, CA). Basal laminar deposit (BLamD) severity and frequency in mice were graded based on a semiquantitative grading system described previously [43].

The thickness of the POS in the toluidine blue–stained sections was measured using the Adobe Photoshop CS4 extended ruler tool at 250 µm interval distances from the optic nerve head. Results of n =3 mice were plotted. POS thickness measurements from the *Atg5*$^{\Delta RPE}$ and *Atg7*$^{\Delta RPE}$ mice were compared with those in the wild-type control mice using the Student *t* test.

Terminal deoxynucleotidyl transferase dUTP nick end labeling (TUNEL) assay was performed for the in situ detection of apoptosis on 10 µm cryosections of mouse eyes using a TACS.XL-Blue Label In Situ Apoptosis Detection Kit (Trevigen, Gaithersburg, MD) according to the manufacturer's instructions.

RESULTS

The gross appearance of the *Atg5*$^{\Delta RPE}$ and *Atg7*$^{\Delta RPE}$ mice was similar to that of wild-type mice. To determine whether RPE-specific deletion of *Atg5* or *Atg7* causes defects in the RPE or the outer retina and whether age is a factor, we examined the ocular phenotype of 20 wild-type, 43 *Atg5*$^{\Delta RPE}$, and 49 *Atg7*$^{\Delta RPE}$ mice from 8 to 24 months of age (Table 1). Because the mouse strain background has been reported to affect some phenotypes of genetically modified mice [40], pigmented (C57BL/6J) and albino (Balb/c) knockout mice (Table 1) were

Table 1. Retinal degeneration in *Atg5*ΔRPE and *Atg7*ΔRPE mice.

Genotype		+/+ (phenotypic/total)		*Atg5*$^{\Delta RPE}$ (phenotypic/total)		*Atg7*$^{\Delta RPE}$ (phenotypic/total)	
Background		Pigmented	Albino	Pigmented	Albino	Pigmented	Albino
Retinal degeneration	8–12 months	0/3	0/3	1/6	2/6	2/9	1/6
	13–18 months	0/3	0/3	2/8	2/7	4/10	3/7
	19–24 months	0/4	0/4	5/9	3/7	7/10	5/7

The number of mice with retinal degeneration out of the total number of mice in each genotype, background, and age group was indicated. Note that more *Atg5*$^{\Delta RPE}$ and *Atg7*$^{\Delta RPE}$ mice showed retinal degeneration as they age. +/+, wild-type controls.

examined. Different background did not affect the RPE or retinal phenotypes we observed.

RPE-specific deletion of Atg5 or Atg7: PCR performed with genomic DNA extracted from isolated RPE cells or the neuroretina confirmed the floxed *Atg5* or *Atg7* fragment is deleted in the RPE but not the neuroretina of the *Atg5*$^{\Delta RPE}$ or *Atg7*$^{\Delta RPE}$ mice. To further validate that there was no *Atg5* or *Atg7* expression in the RPE of these mice, RT–PCR was performed with RNA extracted from isolated RPE cells or the neuroretina. The results showed that no *Atg5* or *Atg7* was expressed in the RPE cells, but both were expressed in the neuroretina isolated from the *Atg5*$^{\Delta RPE}$ or *Atg7*$^{\Delta RPE}$ mice (Figure 1A).

p62/SQSTM1 accumulation in the RPE of Atg5$^{\Delta RPE}$ *and Atg7*$^{\Delta RPE}$ *mice:* p62/SQSTM1 is a cytosolic autophagic adaptor that selectively recognizes autophagic cargo and mediates its engulfment into autophagosomes [44]. The accumulation of p62/SQSTM1 is an indicator of autophagy impairment [44-46]. To assess whether autophagy function was affected in the RPE of the *Atg5*$^{\Delta RPE}$ and *Atg7*$^{\Delta RPE}$ mice, we performed immunofluorescence using frozen sections from 8-month-old mice. Bright fluorescent punctate was observed in the RPE of the *Atg5*$^{\Delta RPE}$ and *Atg7*$^{\Delta RPE}$ mice but not in the wild-type controls (Figure 1B). The p62 fluorescence signal in the RPE was quantified using Image J software. The signal intensity was similar in the RPE of the *Atg5*$^{\Delta RPE}$ and *Atg7*$^{\Delta RPE}$ mice and was nearly double that of the wild-type controls (Figure 1C). This indicates that autophagy in the RPE of the *Atg5*$^{\Delta RPE}$ and *Atg7*$^{\Delta RPE}$ mice was deficient.

Accumulation of oxidatively damaged proteins and DNA in Atg5$^{\Delta RPE}$ *and Atg7*$^{\Delta RPE}$ *mice:* Oxidatively damaged proteins, lipids, and DNA accumulate in the RPE of patients with AMD [12,27,47], trigger complement activation, and contribute to the pathogenesis of macular degeneration [47]. Impaired degradation in the RPE has been suggested to account for the accumulation of oxidative products [11]. Thus, we assessed whether autophagy deficiency induced by RPE-specific deletion of *Atg5* or *Atg7* affects the turnover of oxidized products in the RPE by performing immunofluorescence for markers of oxidation and lipid peroxidation. We found increased levels of 8-OHdG, 3-nitrotyrosine, or AGE fluorescence in the RPE of the *Atg5*$^{\Delta RPE}$ (Figure 2) and *Atg7*$^{\Delta RPE}$ mice (Figure 3). 8-OHdG is one of the predominant forms of free radical-induced oxidative lesions and has been used as a marker for the measurement of endogenous oxidative DNA damage [48]. 3-nitrotyrosine is a product of tyrosine nitration of proteins and is considered a marker of nitric oxide–dependent, reactive nitrogen species–induced oxidative stress [49]. AGEs are proteins or lipids that become glycated by glycation, oxidation, and/or carbonylation [50]. The formation and accumulation of AGEs have been implicated in the progression of age-related diseases [50]. We did not find a difference in the level of HNE or MDA, two markers of lipid peroxidation [51], between the wild-type and the *Atg5*$^{\Delta RPE}$ or *Atg7*$^{\Delta RPE}$ mice. Quantification of marker fluorescence in the RPE showed a greater than 51% increase in 8-OHdG, 3-nitrotyrosine, or AGE in the *Atg5*$^{\Delta RPE}$ and *Atg7*$^{\Delta RPE}$ mice compared with those in the wild-type controls (Figure 4). Increased levels of these markers reflect the accumulation of oxidatively damaged proteins and DNA and indicate that the ability of the RPE to eliminate oxidized wastes was reduced in the *Atg5*$^{\Delta RPE}$ and *Atg7*$^{\Delta RPE}$ mice.

Retinal degeneration in Atg5$^{\Delta RPE}$ *and Atg7*$^{\Delta RPE}$ *mice:* We observed retinal degeneration in 15 *Atg5*$^{\Delta RPE}$ and 22 *Atg7*$^{\Delta RPE}$ mice (Table 1). These mice comprise 35% and 45% of the *Atg5*$^{\Delta RPE}$ and *Atg7*$^{\Delta RPE}$ mice examined, respectively. The number of mice with retinal degeneration increased with age (Table 1). In the *Atg5*$^{\Delta RPE}$ and *Atg7*$^{\Delta RPE}$ mice, the outer plexiform layer (OPL), the outer nuclear layer (ONL), the photoreceptor inner segment (IS), and the POS became thinner with age. These layers were almost completely diminished in some of the mice in the 13- to 18- and 19- to 24-month age groups (Figure 5). Quantification of the POS thickness at 8–12, 13–18, and 19–24 months old showed that

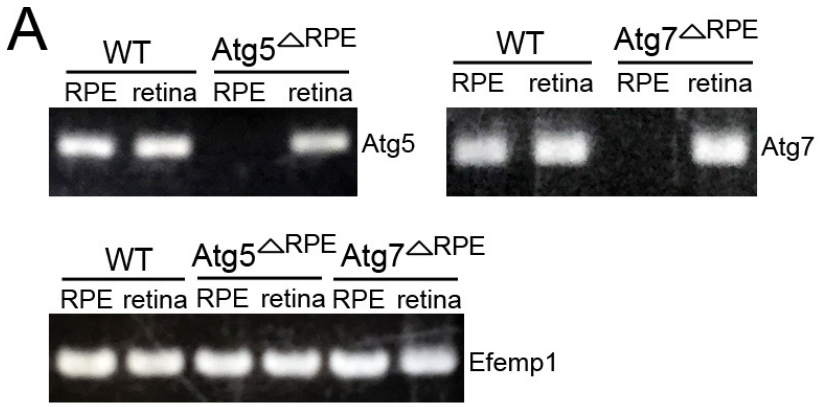

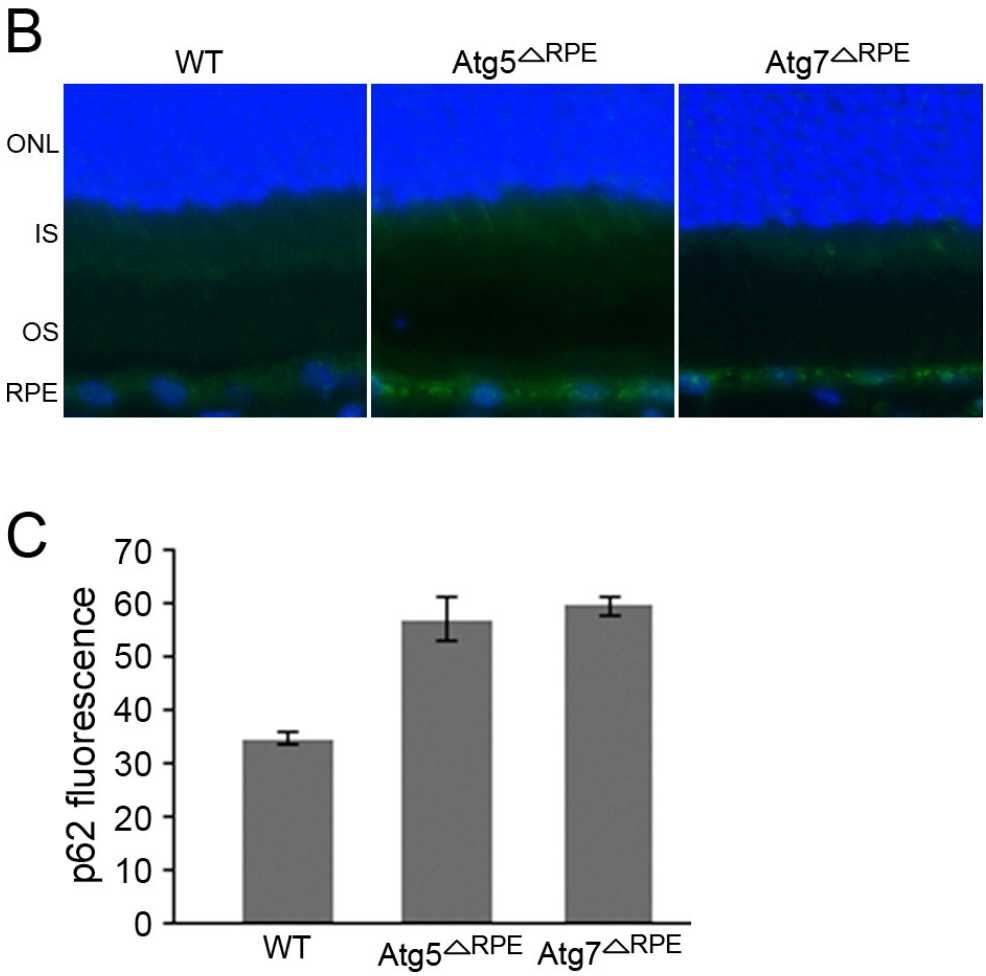

Figure 1. RPE-specific deletion of *Atg5* or *Atg7* and p62/SQSTM1 accumulation in the RPE of *Atg5*$^{\Delta RPE}$ and *Atg7*$^{\Delta RPE}$ mice. **A**: Reverse transcription polymerase chain reaction (RT-PCR) showed that *Atg5* or *Atg7* was not expressed in RPE cells isolated from *Atg5*$^{\Delta RPE}$ or *Atg7*$^{\Delta RPE}$ mice but was expressed in the neuroretina isolated from these mice. RT–PCR using *Efemp1* primers confirmed the integrity of the RNA from all the samples. **B**: Frozen sections from 8-month-old wild-type, *Atg5*$^{\Delta RPE}$, and *Atg7*$^{\Delta RPE}$ mice were stained with an antibody (green signal) against p62/SQSTM1. Note the bright green staining in the RPE of the *Atg5*$^{\Delta RPE}$ and *Atg7*$^{\Delta RPE}$ mice. The nuclei were stained with 4',6-diamidino-2-phenylindole (DAPI; blue signal). **C**: The p62 staining in the RPE was quantified using Image J software. n = 3 mice per genotype. Error bars indicate the mean ± standard deviation (SD). WT, wild-type; ONL, outer nuclear layer; IS, photoreceptor inner segment; OS, photoreceptor outer segment.

degeneration progressed with age (Figure 6). While the POS of the wild-type mice had a mean thickness of about 35 µm at 8–12 months, 30 µm at 13–18 months, and 24 µm at 19–24 months, the POS of the *Atg5*$^{\Delta RPE}$ mice had a mean thickness of about 25 µm, 15 µm, and 3 to 4 µm, respectively. The POS thickness of the *Atg7*$^{\Delta RPE}$ mice was similar to that of the *Atg5*$^{\Delta RPE}$ mice (Figure 6) indicating that the effect of the *Atg5* or *Atg7* deletion was similar. Degeneration of the ONL mirrored that of the POS in terms of age and genotype.

However, we found that the retinal degeneration phenotype was not fully penetrant. Twenty-eight *Atg5*$^{\Delta RPE}$ and 29

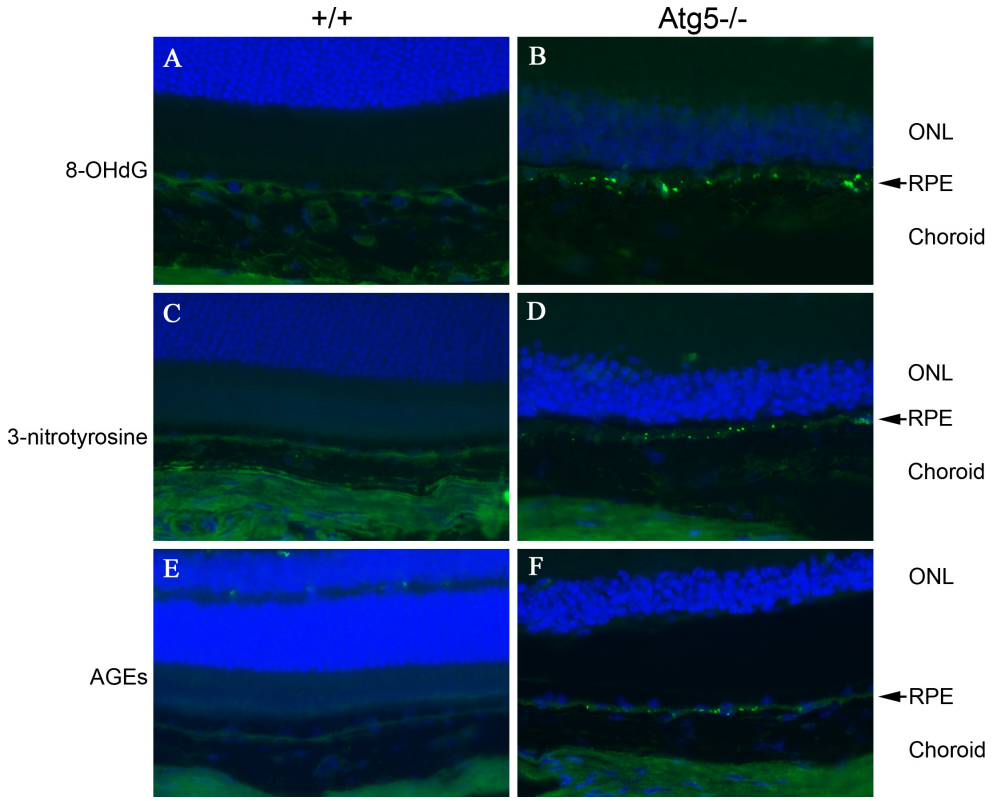

Figure 2. Increased levels of oxidized proteins and DNA in the RPE of aged *Atg5*$^{\Delta RPE}$ mice. Frozen sections from 8-month-old wild-type (+/+; **A**, **C**, **E**) and *Atg5*$^{\Delta RPE}$ (Atg5−/−; **B**, **D**, **F**) mice were stained with antibodies (green signal) against 8-hydroxy-2'-deoxyguanosine (8-OHdG; **A** and **B**), 3-nitrotyrosine (**C** and **D**), or advanced glycation end products (AGEs; **E** and **F**). Note the bright green punctate staining in the RPE of the *Atg5*$^{\Delta RPE}$ mice. The nuclei were stained with 4',6-diamidino-2-phenylindole (DAPI; blue signal).

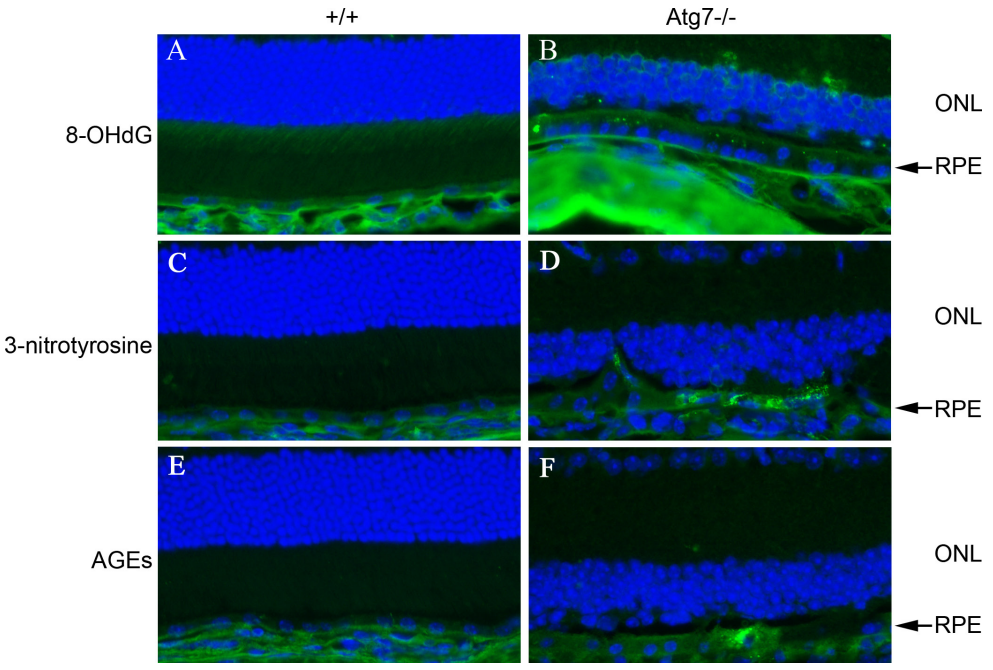

Figure 3. Increased levels of oxidized proteins and DNA in the RPE of aged *Atg7*$^{\Delta RPE}$ mice. Frozen sections from 8-month-old wild-type (+/+; **A**, **C**, **E**) and *Atg7*$^{\Delta RPE}$ (Atg7−/−; **B**, **D**, F) mice were stained with antibodies (green signals) against 8-hydroxy-2'-deoxyguanosine (8-OHdG; **A** and **B**), 3-nitrotyrosine (**C** and **D**), or advanced glycation end products (AGEs; **E** and **F**). Note the bright green staining in the RPE of *Atg7*$^{\Delta RPE}$ mice. The nuclei were stained with 4',6-diamidino-2-phenylindole (DAPI; blue signal).

Atg7$^{\Delta RPE}$ mice examined had normal-appearing retinas and showed no histological signs of degeneration (Figure 5). These results suggest that RPE-specific deletion of *Atg5* or *Atg7* contributes to retinal degeneration but on its own is not sufficient to cause retinal degeneration.

RPE defects in Atg5$^{\Delta RPE}$ *and Atg7*$^{\Delta RPE}$ *mice:* RPE abnormalities similar to the early morphologic features of AMD were found in all the *Atg5*$^{\Delta RPE}$ and *Atg7*$^{\Delta RPE}$ mice with or without retinal degeneration and regardless of the background. The abnormalities ranged from the presence of vacuoles, uneven RPE thickness, diminished basal infoldings, hypertrophy/hypotrophy, and pigmentary irregularities to necrosis (Table 2). The severity of the RPE abnormalities correlated with retinal degeneration and increased with age. In the 8- to 12-month-old *Atg5*$^{\Delta RPE}$ and *Atg7*$^{\Delta RPE}$ mice without retinal degeneration, the only abnormality in the RPE was the presence of vacuoles (Table 2). However, in all age groups of *Atg5*$^{\Delta RPE}$ and *Atg7*$^{\Delta RPE}$ mice with retinal degeneration, all these categories of RPE abnormalities were observed. All these abnormalities were also present in 13- to 18- and 19- to 24-month-old *Atg5*$^{\Delta RPE}$ and *Atg7*$^{\Delta RPE}$ mice without retinal degeneration (Table 2 and Figure 5). When present, the abnormalities were pan retinal.

The thickness of the RPE layer in the *Atg5*$^{\Delta RPE}$ and *Atg7*$^{\Delta RPE}$ mice varied significantly. Mice without retinal degeneration tended to have uneven RPE thickness (Figure 5). Mice with retinal degeneration had an attenuated RPE layer (Figure 7). RPE cells in older mice appeared to be swollen and engorged with pigmented granules (hypertrophy/hyperpigmentation; Figure 5). There were also pale-looking RPE cells with little pigmentation (hypotrophy/hypopigmentation; Figure 7). RPE basal infoldings were scarce and disorganized in the aged *Atg5*$^{\Delta RPE}$ and *Atg7*$^{\Delta RPE}$ mice (Figure 8). RPE cell degeneration reflected by electron dense necrotic cells was observed in some areas of the RPE. We did not detect apoptosis with the TUNEL assays in the RPE in either the *Atg5*$^{\Delta RPE}$ or *Atg7*$^{\Delta RPE}$ mice. In addition to these RPE abnormalities, we found CNV, a late stage complication of AMD, in two *Atg5*$^{\Delta RPE}$ mice (17 and 24 months old) and two *Atg7*$^{\Delta RPE}$ mice (17 and 22 months old) through electron microscopy examination of thin retinal sections (Figure 9). All these mice also had retinal degeneration.

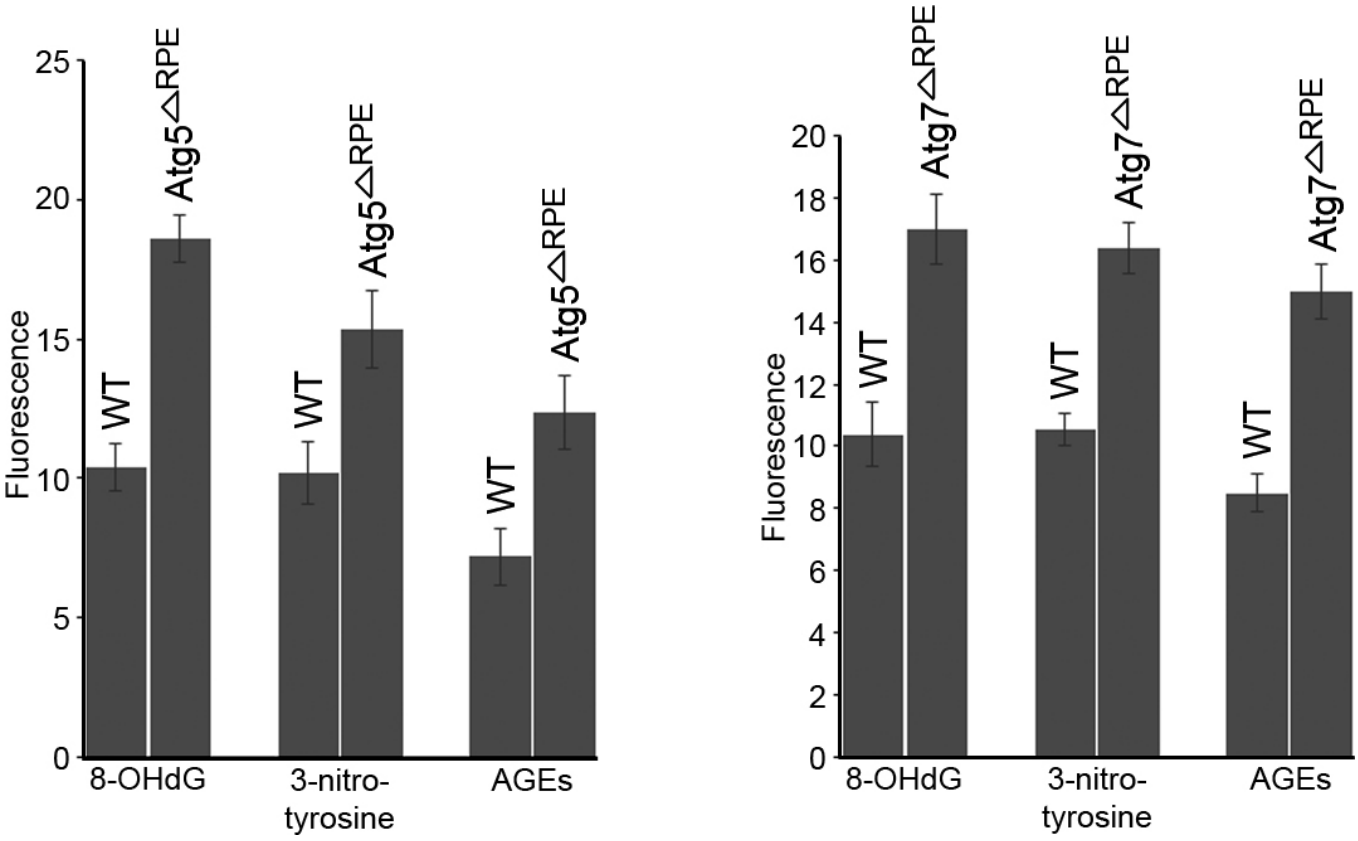

Figure 4. Quantification of 8-OHdG, 3-nitrotyrosine, and AGEs in the RPE of *Atg5*$^{\Delta RPE}$ and *Atg7*$^{\Delta RPE}$ mice. The immunofluorescence staining of 8-OHdG, 3-nitrotyrosine, and advanced glycation end products (AGEs) in the RPE was quantified using Image J software. n = 3 mice per genotype. Error bars indicate the mean ± standard deviation (SD). WT, wild-type control.

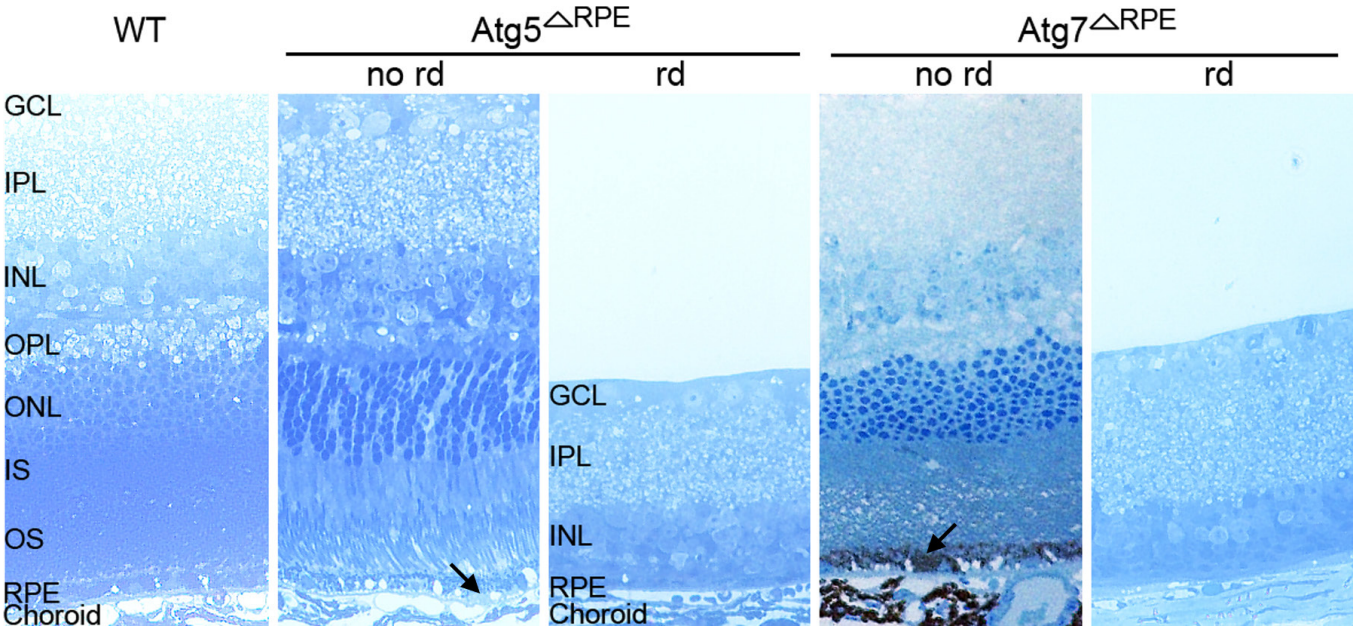

Figure 5. Retinal degeneration in aged *Atg5*$^{\Delta RPE}$ and *Atg7*$^{\Delta RPE}$ mice. Representative images of toluidine blue–stained sections showing the retina layers of 17-month-old wild-type, *Atg5*$^{\Delta RPE}$, and *Atg7*$^{\Delta RPE}$ mice. Note the retina layers of the *Atg5*$^{\Delta RPE}$ and *Atg7*$^{\Delta RPE}$ mice without retinal degeneration (no rd) were similar to those of the wild-type mice but the outer plexiform layer (OPL), ONL, IS, and OS were diminished in the *Atg5*$^{\Delta RPE}$ and *Atg7*$^{\Delta RPE}$ mice with retinal degeneration (rd). The image for the *Atg7*$^{\Delta RPE}$ mice without retinal degeneration was from a pigmented background, and the other images were from albino mice. Arrows indicate engorged RPE cells. GCL, ganglion cell layer; IPL, inner plexiform layer; INL, inner nuclear layer; OPL, outer plexiform layer.

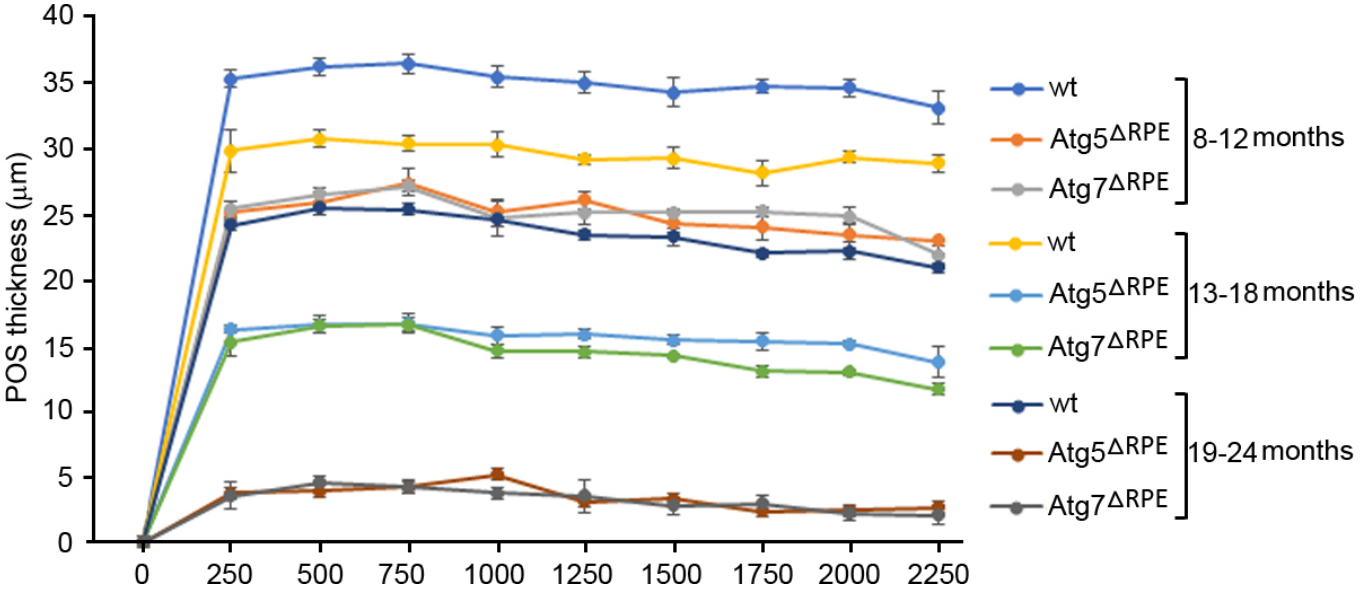

Figure 6. POS thickness in *Atg5*$^{\Delta RPE}$ and *Atg7*$^{\Delta RPE}$ mice with retinal degeneration. The thickness of the photoreceptor outer segment (POS) was measured in the retinas of the mice at 8–12, 13–18, and 19–24 months of age. Each graph represents data from 1 µm toluidine blue–stained sections of three mice (n = 3) per genotype and age group. On each section, nine data points with 250 µm intervals starting from the optic nerve head were measured, and each data point was the mean of three measurements. The value represents the mean of the data points from three mice ± standard deviation (SD). wt, wild-type control mice.

Table 2. RPE abnormalities in *Atg5*$^{\Delta RPE}$ and *Atg7*$^{\Delta RPE}$ mice.

Genotype		*Atg5*$^{\Delta RPE}$		*Atg7*$^{\Delta RPE}$	
Retinal degeneration		-	+	-	+
Vacuoles	8–12 months	+	+	+	+
	13–18 months	+	+	+	+
	19–24 months	+	+	+	+
Uneven RPE thickness	8–12 months	-	+	-	+
	13–18 months	+	+	+	+
	19–24 months	+	+	+	+
Loss of basal infoldings	8–12 months	-	+	-	+
	13–18 months	+	+	+	+
	19–24 months	+	+	+	+
Hypertrophy / hypotrophy	8–12 months	-	+	-	+
	13–18 months	+	+	+	+
	19–24 months	+	+	+	+
Pigmentary irregularities	8–12 months	-	+	-	+
	13–18 months	+	+	+	+
	19–24 months	+	+	+	+
Necrosis	8–12 months	-	+	-	+
	13–18 months	+	+	+	+
	19–24 months	+	+	+	+

RPE abnormalities observed in *Atg5*$^{\Delta RPE}$ and *Atg7*$^{\Delta RPE}$ mice aging from 8 to 24 months were classified into six categories. "-" indicates no difference between *Atg5*$^{\Delta RPE}$/*Atg7*$^{\Delta RPE}$ and age-matched wild-type control mice; and "+" indicates abnormalities in *Atg5*$^{\Delta RPE}$ or *Atg7*$^{\Delta RPE}$ mice

No sub-RPE deposits in Atg5$^{\Delta RPE}$ *and Atg7*$^{\Delta RPE}$ *mice:* Sub-RPE deposits are strongly associated with AMD. In the mouse, BLamD is the main form of sub-RPE deposits. We thus examined whether BLamDs were present in *Atg5*$^{\Delta RPE}$ and *Atg7*$^{\Delta RPE}$ mice. We adapted a semiquantitative grading system to grade BLamD severity and frequency [43,52]. Based on this system, mild BLamD referred to the presence of any discrete focal nodule of homogenous deposit between the RPE cell membrane and its basement membrane in at least one micrograph (of at least ten) within a section from an individual specimen [43]. Only small isolated BLamDs were seen occasionally in the *Atg5*$^{\Delta RPE}$ and *Atg7*$^{\Delta RPE}$ mice at 19–24 months old. The severity and frequency of BLamDs in these mice were similar to those of the age-matched wild-type controls and did not reach the "mild BLamD" category. This finding indicates that BLamD was not induced by RPE-specific deletion of *Atg5* or *Atg7*.

DISCUSSION

RPE dysfunction and aging are two main risk factors for AMD and other forms of retinal degeneration. In this study, we analyzed the effect of autophagy deficiency in the RPE that resulted from murine *Atg5* or *Atg7* deletion with advanced age. We found that RPE-specific deletion of *Atg5* or *Atg7* impairs the RPE's waste-removing capacity, accelerates the accumulation of oxidized waste, and leads to early AMD-like RPE defects and partially penetrant retinal degeneration. RPE cells are non-dividing cells with an innate capacity to clear the large amount of metabolic waste generated by photoreceptors in the outer retina. The effect of autophagy deficiency appears to take time to manifest and is most evident in aged *Atg5*$^{\Delta RPE}$ and *Atg7*$^{\Delta RPE}$ mice. Mice younger than 6 months did not exhibit obvious defects in the RPE or the outer retina. This suggests that RPE cells can function for at least a limited time with deficient autophagy.

The RPE abnormalities found in the aged *Atg5*$^{\Delta RPE}$ and *Atg7*$^{\Delta RPE}$ mice are similar to the RPE cellular features of early AMD [11,12,21]. However, we did not find sub-RPE deposits, a characteristic early feature of typical AMD [21,23,24], in these mice. Some patients with AMD do not have sub-RPE deposits [53]. The present data suggest that autophagy deficiency contributes to the pathogenesis of AMD by affecting the biochemical pathway(s) that are not involved in the formation of sub-RPE deposits. Although it is still not clear how sub-RPE deposits form, a plausible hypothesis is that chronic inflammation triggered by oxidatively modified lipids in Bruch's membrane leads to deposit formation [47]. Interestingly, we did not find increased levels of lipid peroxidation marker HNE or MDA in either the *Atg5*$^{\Delta RPE}$ or *Atg7*$^{\Delta RPE}$ mice. Accumulation of 3-nitrotyrosine, AGEs, and 8-OHdG in the RPE of these mice suggests that autophagy deficiency affects their turnover in the RPE but not their accumulation in sub-RPE deposits.

RPE thinning to atrophy was found in aged *Atg5*$^{\Delta RPE}$ and *Atg7*$^{\Delta RPE}$ mice with retinal degeneration. When an RPE cell dies, the nearby cells clear the body and stretch to cover the space. This results in thinned, hypopigmented cells. When the cells can no longer stretch to fill the gap, atrophy occurs [21]. RPE atrophy is a feature of late stage dry AMD [21]. CNV was occasionally found in aged *Atg5*$^{\Delta RPE}$ and *Atg7*$^{\Delta RPE}$ mice with retinal degeneration. In wet AMD, CNV is a late stage feature [24]. The present findings suggest that autophagy deficiency contributes to disease progression in AMD.

AMD and retinal degeneration are complex multifactorial diseases. Variation in the severity of RPE defects and partially penetrant retinal degeneration in *Atg5*$^{\Delta RPE}$ and *Atg7*$^{\Delta RPE}$ mice suggest that *Atg5*- or *Atg7*-dependent autophagy

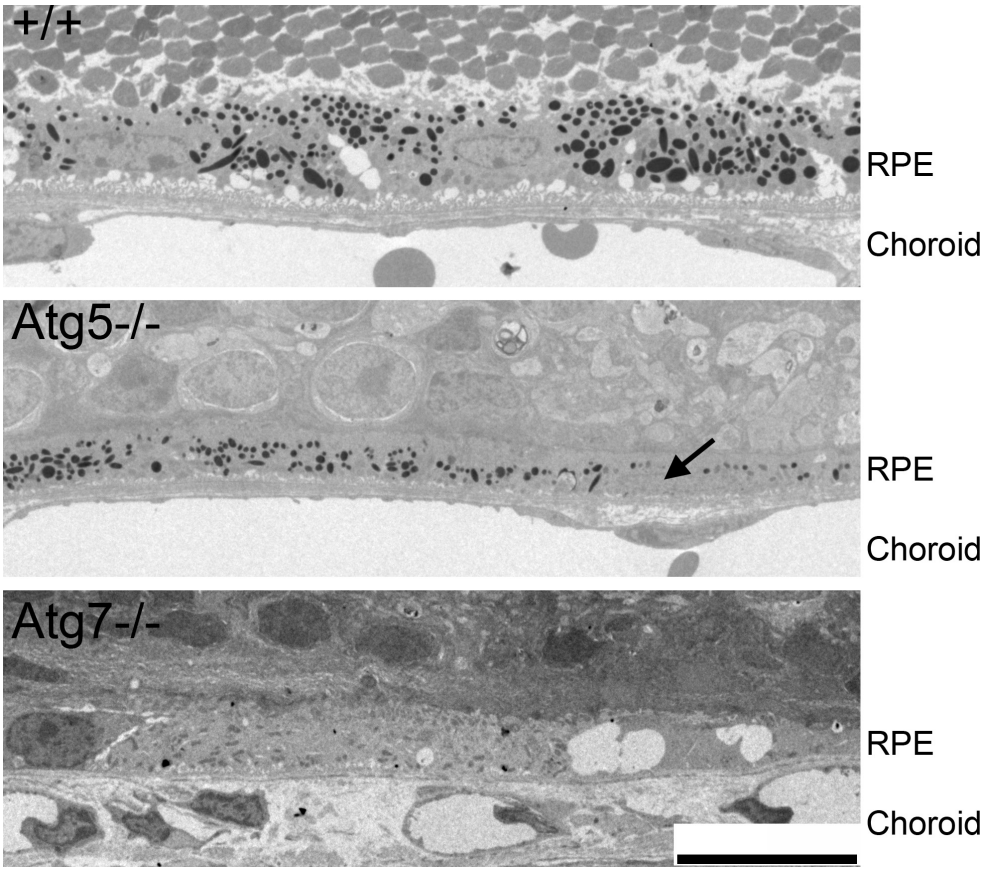

Figure 7. Thinned RPE in aged *Atg5*$^{\Delta RPE}$ and *Atg7*$^{\Delta RPE}$ mice. Representative electronic micrographs showing the RPE region of the 17-month-old wild-type (+/+), *Atg5*$^{\Delta RPE}$ (Atg5−/−), and *Atg7*$^{\Delta RPE}$ (Atg7−/−) mice. Note that the RPE thicknesses of the *Atg5*$^{\Delta RPE}$ and *Atg7*$^{\Delta RPE}$ mice are approximately one third to one half that of the wild-type mice. The wild-type and *Atg5*$^{\Delta RPE}$ mice shown were pigmented, and the *Atg7*$^{\Delta RPE}$ mouse was albino. Arrow indicates a hypotrophic RPE cell. Scale bar = 10 µm.

is only one contributing factor in the pathogenesis of these diseases. Manifestation of disease may require the collapse of several RPE cellular functions simultaneously, especially in the case of retinal degeneration. More than half of the *Atg5*$^{\Delta RPE}$ and *Atg7*$^{\Delta RPE}$ mice at 8 to 24 months old did not show any histological sign of retinal degeneration. This suggests that RPE-specific deletion of *Atg5* or *Atg7* in these mice did not tip over the balance maintained by other stress and anti-stress factors. RPE defects were more severe in the *Atg5*$^{\Delta RPE}$ and *Atg7*$^{\Delta RPE}$ mice with retinal degeneration suggesting that these mice are dealing with more overall stress. The number of *Atg5*$^{\Delta RPE}$ and *Atg7*$^{\Delta RPE}$ mice showing retinal degeneration increased with age, and the severity of degeneration also increased with age. It is likely that *Atg5* or *Atg7* deletion adds stress to the RPE, but disease occurs only when the overall stress from other factors increases above a certain threshold as the mouse ages. In the *Atg5*$^{\Delta RPE}$ and *Atg7*$^{\Delta RPE}$ mice without retinal degeneration, the overall stress never exceeded the disease threshold.

Several other studies involving the RPE-specific deletion of murine *Atg5* or *Atg7* did not report retinal degeneration [33-35]. Kim et al. found that *Atg5* loss in the RPE resulted

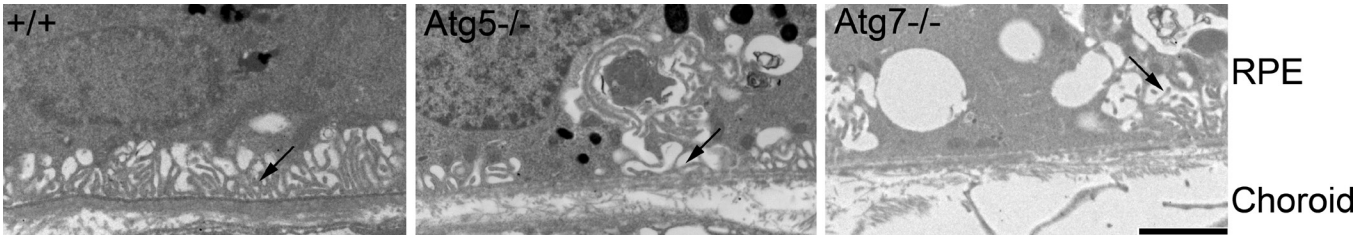

Figure 8. Diminished RPE basal infoldings in aged *Atg5*$^{\Delta RPE}$ and *Atg7*$^{\Delta RPE}$ mice. Representative electronic micrographs showing the RPE basal infolding area of 17-month-old wild-type (+/+), *Atg5*$^{\Delta RPE}$ (Atg5−/−), and *Atg7*$^{\Delta RPE}$ (Atg7−/−) mice. Note the scarce basal infoldings (arrow) in the *Atg5*$^{\Delta RPE}$ and *Atg7*$^{\Delta RPE}$ mice. Scale bar = 2 µm.

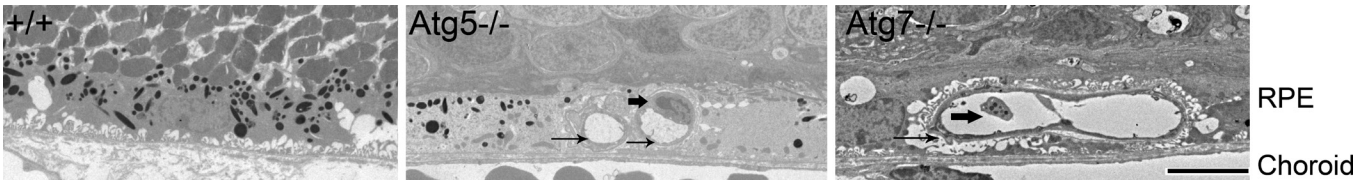

Figure 9. CNV in aged *Atg5*$^{\Delta RPE}$ and *Atg7*$^{\Delta RPE}$ mice. Representative electronic micrographs showing the RPE area of 17-month-old wild-type (+/+), *Atg5*$^{\Delta RPE}$ (Atg5−/−), and *Atg7*$^{\Delta RPE}$ (Atg7−/−) mice. Note the blood vessels (thin arrows) in the RPE layer of the *Atg5*$^{\Delta RPE}$ or *Atg7*$^{\Delta RPE}$ mice. Thick arrow indicates a capillary endothelial cell (Atg5−/−) or a platelet (Atg7−/−). Scale bar = 5 µm.

in disrupted lysosomal processing, decreased photoreceptor responses to light stimuli, decreased chromophore levels, but no detectable decrease in the numbers of photoreceptors up to 1.5 years of age [33]. Mice with tyrosinase-cre-mediated deletion of *Atg7* had accumulation of autophagy substrates and the RPE65 variant M450 accompanied by increased expression of other regulators of the visual cycle but showed no signs of visual impairment up to 2 years of age [35]. Perusek et al. reported that mice with the *Atg7* deletion in the RPE had abnormal RPE morphology with RPE hypertrophy, cellular debris, and vacuole formation [34]. These mice had trouble coping with stress caused by di-retinoid-pyridinium-ethanolamine (A2E) accumulation but did not show higher amounts of A2E in the RPE or retinal degeneration at 6 and 12 months old [34]. These studies are consistent with our conclusion that RPE-specific deletion of *Atg5* or *Atg7* alone is not sufficient to induce retinal degeneration. In their studies, the overall stress in the *Atg5*$^{\Delta RPE}$ or *Atg7*$^{\Delta RPE}$ mice did not exceed the disease threshold. Because we examined a large number of aged mice at different time points for retinal degeneration, we were able to observe retinal degeneration in a portion of mice, especially with advanced age.

In this study, the autophagy deficiency in the RPE is induced by the deletion of *Atg5* or *Atg7*, two core components of the conventional autophagy pathway. Recently, an Atg5/Atg7-independent alternative pathway has been reported [54]. This alternative pathway is regulated by some components of the conventional autophagy pathway, including Unc-51-like kinase 1 (Ulk1) and beclin 1, but is also dependent on some proteins that had previously not been associated with autophagy, such as Rab9 [54]. Although conventional and alternative processes lead to the bulk degradation of subcellular constituents, they may be activated by different stimuli in different cell types and may have different physiologic functions. It is possible that in the absence of Atg5 or Atg7, an alternative autophagy pathway is upregulated and prevents retinal degeneration in some *Atg5*$^{\Delta RPE}$ or *Atg7*$^{\Delta RPE}$ mice.

In summary, our data show that defects in autophagy predispose to but do not necessarily drive the development of AMD-like phenotypes or retinal degeneration. Other risk factors, such as aging, augment the effect of autophagy deficiency in the pathogenesis of these diseases.

ACKNOWLEDGMENTS

We are grateful to Lori A. Bachman and Benjamin J. Gilles for assistance in mouse care, Dr. Adiv A. Johnson for technical assistance, and the staff in the electron microscopy core facility at the Mayo Clinic for their assistance with transmission electron microscopy. This work was supported by NIH grants R01EY0013847 (LYM), R01EY0013160 (ADM), and R01EY0021153 (ADM), Mayo Foundation, and an unrestricted grant from Research to Prevent Blindness to the Department of Ophthalmology at the Mayo Clinic in Rochester, Minnesota.

REFERENCES

1. Strauss O. The retinal pigment epithelium in visual function. Physiol Rev 2005; 85:845-81. [PMID: 15987797].
2. Bok D. The retinal pigment epithelium: a versatile partner in vision. J Cell Sci Suppl 1993; 17:189-95. [PMID: 8144697].
3. Rubinsztein DC, DiFiglia M, Heintz N, Nixon RA, Qin ZH, Ravikumar B, Stefanis L, Tolkovsky A. Autophagy and its possible roles in nervous system diseases, damage and repair. Autophagy 2005; 1:11-22. [PMID: 16874045].
4. Levine B, Kroemer G. Autophagy in the pathogenesis of disease. Cell 2008; 132:27-42. [PMID: 18191218].
5. Xie Z, Klionsky DJ. Autophagosome formation: core machinery and adaptations. Nat Cell Biol 2007; 9:1102-9. [PMID: 17909521].
6. Mizushima N, Levine B, Cuervo AM, Klionsky DJ. Autophagy fights disease through cellular self-digestion. Nature 2008; 451:1069-75. [PMID: 18305538].
7. Vellai T. Autophagy genes and ageing. Cell Death Differ 2009; 16:94-102. [PMID: 19079287].
8. Sarkar S, Rubinsztein DC. Small molecule enhancers of autophagy for neurodegenerative diseases. Mol Biosyst 2008; 4:895-901. [PMID: 18704227].

9. Sarkar S, Rubinsztein DC. Huntington's disease: degradation of mutant huntingtin by autophagy. FEBS J 2008; 275:4263-70. [PMID: 18637946].

10. Fornai F, Longone P, Cafaro L, Kastsiuchenka O, Ferrucci M, Manca ML, Lazzeri G, Spalloni A, Bellio N, Lenzi P, Modugno N, Siciliano G, Isidoro C, Murri L, Ruggieri S, Paparelli A. Lithium delays progression of amyotrophic lateral sclerosis. Proc Natl Acad Sci USA 2008; 105:2052-7. [PMID: 18250315].

11. de Jong PT. Age-related macular degeneration. N Engl J Med 2006; 355:1474-85. [PMID: 17021323].

12. Beatty S, Koh H, Phil M, Henson D, Boulton M. The role of oxidative stress in the pathogenesis of age-related macular degeneration. Surv Ophthalmol 2000; 45:115-34. [PMID: 11033038].

13. Mitter SK, Rao HV, Qi X, Cai J, Sugrue A, Dunn WA Jr, Grant MB, Boulton ME. Autophagy in the retina: a potential role in age-related macular degeneration. Adv Exp Med Biol 2012; 723:83-90. [PMID: 22183319].

14. Athanasiou D, Aguila M, Bevilacqua D, Novoselov SS, Parfitt DA, Cheetham ME. The cell stress machinery and retinal degeneration. FEBS Lett 2013; 587:2008-17. [PMID: 23684651].

15. Kaarniranta K, Sinha D, Blasiak J, Kauppinen A, Vereb Z, Salminen A, Boulton ME, Petrovski G. Autophagy and heterophagy dysregulation leads to retinal pigment epithelium dysfunction and development of age-related macular degeneration. Autophagy 2013; 9:973-84. [PMID: 23590900].

16. Sinha D, Valapala M, Shang P, Hose S, Grebe R, Lutty GA, Zigler JS Jr, Kaarniranta K, Handa JT. Lysosomes: Regulators of autophagy in the retinal pigmented epithelium. Exp Eye Res 2016; 144:46-53. [PMID: 26321509].

17. Boya P, Esteban-Martinez L, Serrano-Puebla A, Gomez-Sintes R, Villarejo-Zori B. Autophagy in the eye: Development, degeneration, and aging. Prog Retin Eye Res 2016; 55:206-45. [PMID: 27566190].

18. Wang AL, Lukas TJ, Yuan M, Du N, Tso MO, Neufeld AH. Autophagy and exosomes in the aged retinal pigment epithelium: possible relevance to drusen formation and age-related macular degeneration. PLoS One 2009; 4:e4160-[PMID: 19129916].

19. Evans JR, Fletcher AE, Wormald RP. Age-related macular degeneration causing visual impairment in people 75 years or older in Britain: an add-on study to the Medical Research Council Trial of Assessment and Management of Older People in the Community. Ophthalmology 2004; 111:513-7. [PMID: 15019328].

20. Buschini E, Piras A, Nuzzi R, Vercelli A. Age related macular degeneration and drusen: neuroinflammation in the retina. Prog Neurobiol 2011; 95:14-25. [PMID: 21740956].

21. Sarks SH, Sarks JP. Age-related maculopathy: Nonneovascular age-related macular degeneration and the evolution of geographic atrophy. In Ryan SJ (ed): "Retina." St. Louis: Mosby, 2001:1064.

22. Feher J, Kovacs I, Artico M, Cavallotti C, Papale A, Balacco Gabrieli C. Mitochondrial alterations of retinal pigment epithelium in age-related macular degeneration. Neurobiol Aging 2006; 27:983-93. [PMID: 15979212].

23. Green WR. Histopathology of age-related macular degeneration. Mol Vis 1999; 5:27-36. [PMID: 10562651].

24. Bressler NM, Silva JC, Bressler SB, Fine SL, Green WR. Clinicopathologic correlation of drusen and retinal pigment epithelial abnormalities in age-related macular degeneration. Retina 1994; 14:130-42. [PMID: 8036323].

25. Crabb JW, Miyagi M, Gu X, Shadrach K, West KA, Sakaguchi H, Kamei M, Hasan A, Yan L, Rayborn ME, Salomon RG, Hollyfield JG. Drusen proteome analysis: an approach to the etiology of age-related macular degeneration. Proc Natl Acad Sci USA 2002; 99:14682-7. [PMID: 12391305].

26. Umeda S, Suzuki MT, Okamoto H, Ono F, Mizota A, Terao K, Yoshikawa Y, Tanaka Y, Iwata T. Molecular composition of drusen and possible involvement of anti-retinal autoimmunity in two different forms of macular degeneration in cynomolgus monkey (Macaca fascicularis). FASEB J 2005; 19:1683-5. [PMID: 16099945].

27. Schutt F, Bergmann M, Holz FG, Kopitz J. Proteins modified by malondialdehyde, 4-hydroxynonenal, or advanced glycation end products in lipofuscin of human retinal pigment epithelium. Invest Ophthalmol Vis Sci 2003; 44:3663-8. [PMID: 12882821].

28. Hirata A, Feeney-Burns L. Autoradiographic studies of aged primate macular retinal pigment epithelium. Invest Ophthalmol Vis Sci 1992; 33:2079-90. [PMID: 1607221].

29. Anderson DH, Mullins RF, Hageman GS, Johnson LV. A role for local inflammation in the formation of drusen in the aging eye. Am J Ophthalmol 2002; 134:411-31. [PMID: 12208254].

30. Noda NN, Inagaki F. Mechanisms of Autophagy. Annu Rev Biophys 2015; 44:101-22. [PMID: 25747593].

31. Kuma A, Hatano M, Matsui M, Yamamoto A, Nakaya H, Yoshimori T, Ohsumi Y, Tokuhisa T, Mizushima N. The role of autophagy during the early neonatal starvation period. Nature 2004; 432:1032-6. [PMID: 15525940].

32. Komatsu M, Waguri S, Ueno T, Iwata J, Murata S, Tanida I, Ezaki J, Mizushima N, Ohsumi Y, Uchiyama Y, Kominami E, Tanaka K, Chiba T. Impairment of starvation-induced and constitutive autophagy in Atg7-deficient mice. J Cell Biol 2005; 169:425-34. [PMID: 15866887].

33. Kim JY, Zhao H, Martinez J, Doggett TA, Kolesnikov AV, Tang PH, Ablonczy Z, Chan CC, Zhou Z, Green DR, Ferguson TA. Noncanonical autophagy promotes the visual cycle. Cell 2013; 154:365-76. [PMID: 23870125].

34. Perusek L, Sahu B, Parmar T, Maeno H, Arai E, Le YZ, Subauste CS, Chen Y, Palczewski K, Maeda A. Di-retinoid-pyridinium-ethanolamine (A2E) Accumulation and the Maintenance of the Visual Cycle Are Independent of

Atg7-mediated Autophagy in the Retinal Pigmented Epithelium. J Biol Chem 2015; 290:29035-44. [PMID: 26468292].

35. Sukseree S, Chen YT, Laggner M, Gruber F, Petit V, Nagelreiter IM, Mlitz V, Rossiter H, Pollreisz A, Schmidt-Erfurth U, Larue L, Tschachler E, Eckhart L. Tyrosinase-Cre-Mediated Deletion of the Autophagy Gene Atg7 Leads to Accumulation of the RPE65 Variant M450 in the Retinal Pigment Epithelium of C57BL/6 Mice. PLoS One 2016; 11:e0161640-[PMID: 27537685].

36. Hara T, Nakamura K, Matsui M, Yamamoto A, Nakahara Y, Suzuki-Migishima R, Yokoyama M, Mishima K, Saito I, Okano H, Mizushima N. Suppression of basal autophagy in neural cells causes neurodegenerative disease in mice. Nature 2006; 441:885-9. [PMID: 16625204].

37. Le YZ, Zheng W, Rao PC, Zheng L, Anderson RE, Esumi N, Zack DJ, Zhu M. Inducible expression of cre recombinase in the retinal pigmented epithelium. Invest Ophthalmol Vis Sci 2008; 49:1248-53. [PMID: 18326755].

38. Marmorstein AD, Marmorstein LY, Rayborn M, Wang X, Hollyfield JG, Petrukhin K. Bestrophin, the product of the Best vitelliform macular dystrophy gene (VMD2), localizes to the basolateral plasma membrane of the retinal pigment epithelium. Proc Natl Acad Sci USA 2000; 97:12758-63. [PMID: 11050159].

39. Esumi N, Oshima Y, Li Y, Campochiaro PA, Zack DJ. Analysis of the VMD2 promoter and implication of E-box binding factors in its regulation. J Biol Chem 2004; 279:19064-73. [PMID: 14982938].

40. McLaughlin PJ, Bakall B, Choi J, Liu Z, Sasaki T, Davis EC, Marmorstein AD, Marmorstein LY. Lack of fibulin-3 causes early aging and herniation, but not macular degeneration in mice. Hum Mol Genet 2007; 16:3059-70. [PMID: 17872905].

41. McLaughlin PJ, Chen Q, Horiguchi M, Starcher BC, Stanton JB, Broekelmann TJ, Marmorstein AD, McKay B, Mecham R, Nakamura T, Marmorstein LY. Targeted disruption of fibulin-4 abolishes elastogenesis and causes perinatal lethality in mice. Mol Cell Biol 2006; 26:1700-9. [PMID: 16478991].

42. Marmorstein LY, McLaughlin PJ, Peachey NS, Sasaki T, Marmorstein AD. Formation and progression of sub-retinal pigment epithelium deposits in Efemp1 mutation knock-in mice: a model for the early pathogenic course of macular degeneration. Hum Mol Genet 2007; 16:2423-32. [PMID: 17664227].

43. Stanton JB, Marmorstein AD, Zhang Y, Marmorstein LY. Deletion of Efemp1 Is Protective Against the Development of Sub-RPE Deposits in Mouse Eyes. Invest Ophthalmol Vis Sci 2017; 58:1455-61. [PMID: 28264101].

44. Katsuragi Y, Ichimura Y, Komatsu M. p62/SQSTM1 functions as a signaling hub and an autophagy adaptor. FEBS J 2015; 282:4672-8. [PMID: 26432171].

45. Komatsu M, Waguri S, Koike M, Sou YS, Ueno T, Hara T, Mizushima N, Iwata J, Ezaki J, Murata S, Hamazaki J, Nishito Y, Iemura S, Natsume T, Yanagawa T, Uwayama J, Warabi E, Yoshida H, Ishii T, Kobayashi A, Yamamoto M, Yue Z, Uchiyama Y, Kominami E, Tanaka K. Homeostatic levels of p62 control cytoplasmic inclusion body formation in autophagy-deficient mice. Cell 2007; 131:1149-63. [PMID: 18083104].

46. Bjorkoy G, Lamark T, Pankiv S, Øvervatn A, Brech A, Johansen T. Monitoring autophagic degradation of p62/SQSTM1. Methods Enzymol 2009; 452:181-97. [PMID: 19200883].

47. Handa JT, Cano M, Wang L, Datta S, Liu T. Lipids, oxidized lipids, oxidation-specific epitopes, and Age-related Macular Degeneration. Biochim Biophys Acta 2017; xxx:430-40. .

48. Valavanidis A, Vlachogianni T, Fiotakis C. 8-hydroxy-2′ -deoxyguanosine (8-OHdG): A critical biomarker of oxidative stress and carcinogenesis. J Environ Sci Health C Environ Carcinog Ecotoxicol Rev 2009; 27:120-39. [PMID: 19412858].

49. Pacher P, Beckman JS, Liaudet L. Nitric oxide and peroxynitrite in health and disease. Physiol Rev 2007; 87:315-424. [PMID: 17237348].

50. Vistoli G, De Maddis D, Cipak A, Zarkovic N, Carini M, Aldini G. Advanced glycoxidation and lipoxidation end products (AGEs and ALEs): an overview of their mechanisms of formation. Free Radic Res 2013; 47:Suppl 13-27. [PMID: 23767955].

51. Ayala A, Munoz MF, Arguelles S. Lipid peroxidation: production, metabolism, and signaling mechanisms of malondialdehyde and 4-hydroxy-2-nonenal. Oxid Med Cell Longev 2014; 2014:360438-.

52. Cousins SW, Espinosa-Heidmann DG, Alexandridou A, Sall J, Dubovy S, Csaky K. The role of aging, high fat diet and blue light exposure in an experimental mouse model for basal laminar deposit formation. Exp Eye Res 2002; 75:543-53. [PMID: 12457866].

53. Bird AC, Bressler NM, Bressler SB, Chisholm IH, Coscas G, Davis MD, de Jong PT, Klaver CC, Klein BE, Klein R, Mitchell P, Sarks JP, Sarks SH, Soubrane G, Taylor HR, Vingerling JR. An international classification and grading system for age-related maculopathy and age-related macular degeneration. The International ARM Epidemiological Study Group. Surv Ophthalmol 1995; 39:367-74. .

54. Nishida Y, Arakawa S, Fujitani K, Yamaguchi H, Mizuta T, Kanaseki T, Komatsu M, Otsu K, Tsujimoto Y, Shimizu S. Discovery of Atg5/Atg7-independent alternative macroautophagy. Nature 2009; 461:654-8. [PMID: 19794493].

Articles are provided courtesy of Emory University and the Zhongshan Ophthalmic Center, Sun Yat-sen University, P.R. China. The print version of this article was created on 14 April 2017. This reflects all typographical corrections and errata to the article through that date. Details of any changes may be found in the online version of the article.